Electronic Supplementary Information

Oxygen-Powered Flower-like $FeMo_6@CeO_2$ Self-cascade Nanozyme: Turn-on Enhancement Fluorescence Sensor

Zhibo Tong,[a] Tong Wang,[b] Yunheng Cai,[b] Jingquan Sha*[b], Tai Peng*[a]

[a] College of Materials Science and Engineering, Jiamusi University, HeilongJiang, Jiamusi, 154007, P.R. China
[b] School of Chemistry, Chemical Engineering and Materials, Jining University, Shandong, Qufu 273155, P. R. China
*Corresponding author: E-mail address: pt@jmsu.edu.cn.

Table of Contents

Section 1. Supporting Figures

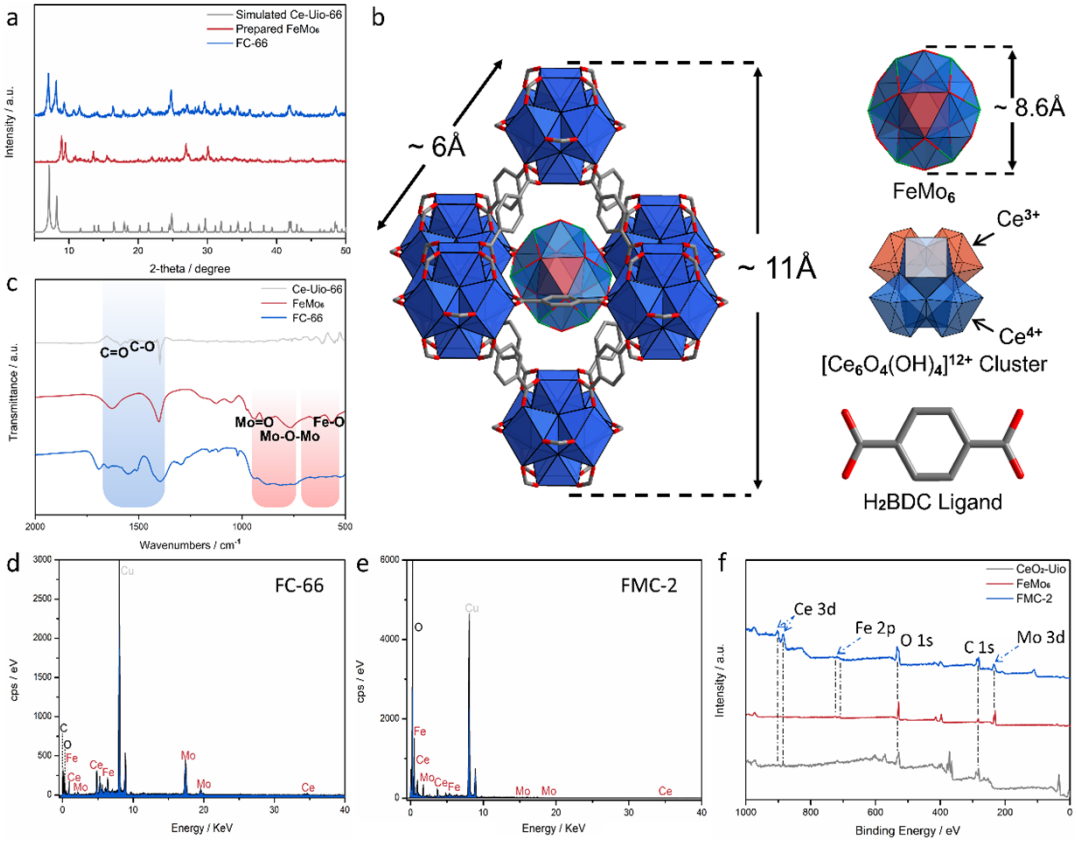

Figure S1. (a) XRD pattern observed for FC-66 in comparison with the prepared $FeMo_6$ as well as the simulated pattern of Ce-Uio-66; (b) combined wires/sticks/polyhedral representation of the asymmetric unit of FC-66; (c) the FT-IR spectra of Ce-Uio-66, $FeMo_6$ and FC-66; EDS spectrums of (d) FC-66 and (e) FMC-2; (f) full survey scan of XPS spectra for FMC-2, $FeMo_6$ and CeO_2-Uio, respectively.

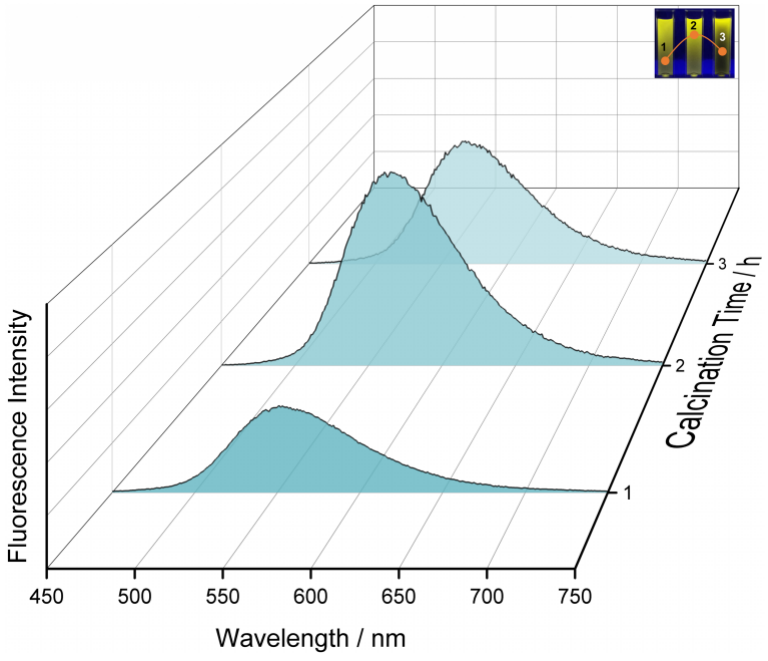

Figure S2 Fluorescence curves and optical photographs of FMC-n.

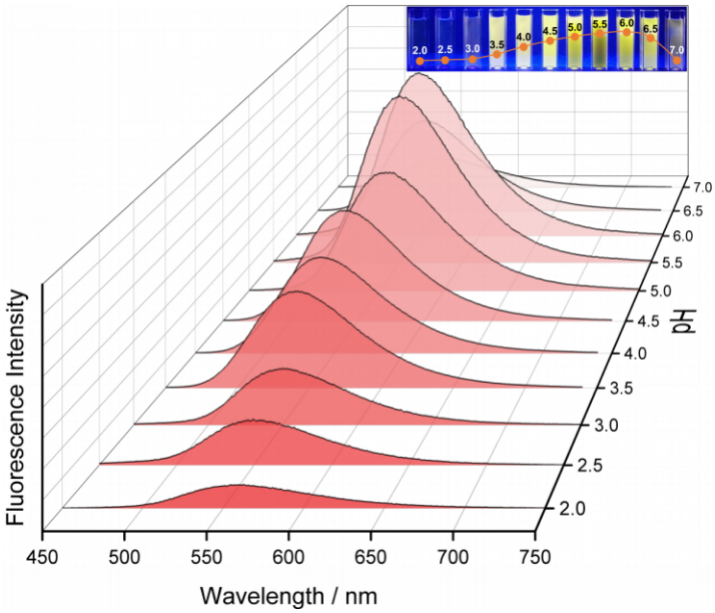

Figure S3 Fluorescence curves and optical photos of FMC-2 under different pH.

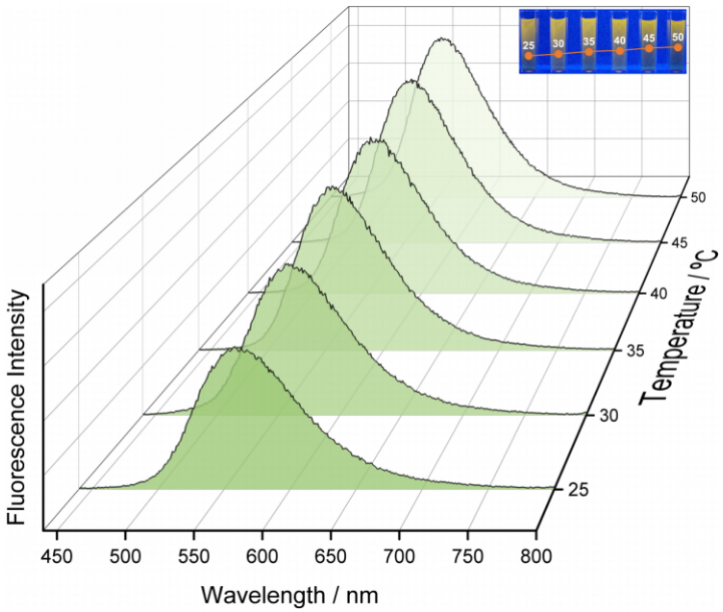

Figure S4 Fluorescence curves and optical photos of FMC-2 under different temperatures.

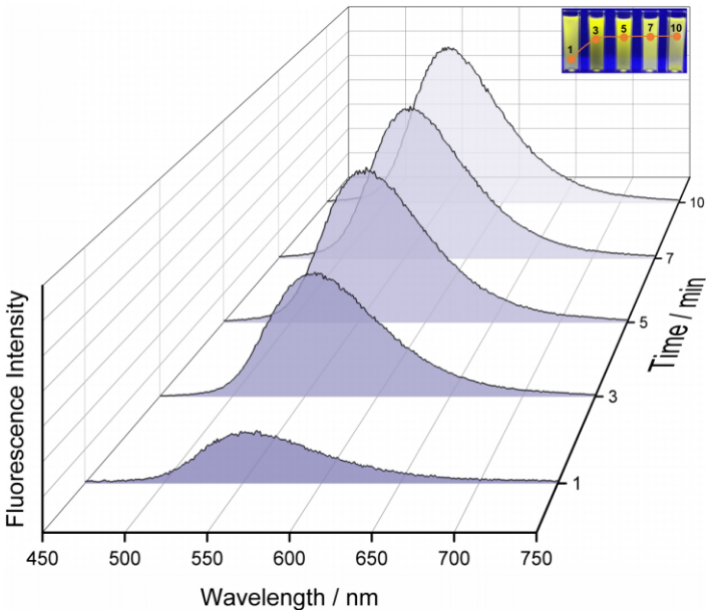

Figure S5 Fluorescence curves and optical photos of FMC-2 under different reaction times.

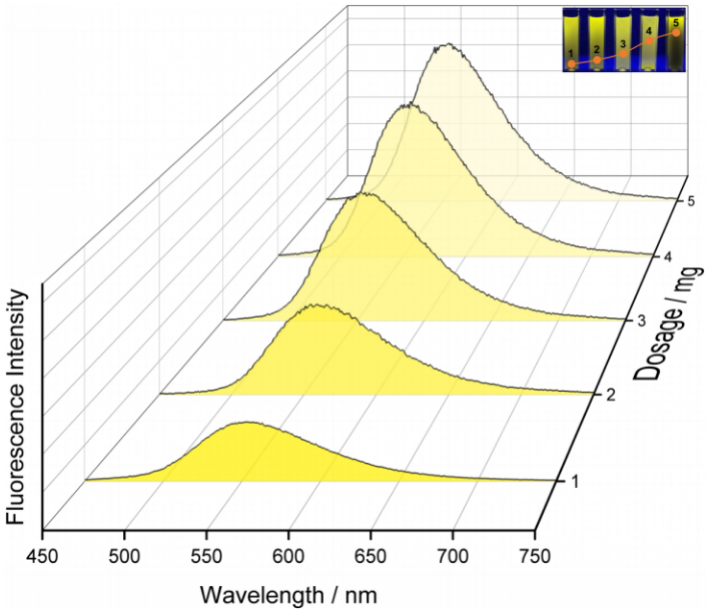

Figure S6 Fluorescence curves and optical photos of FMC-2 with different feeding dosage.

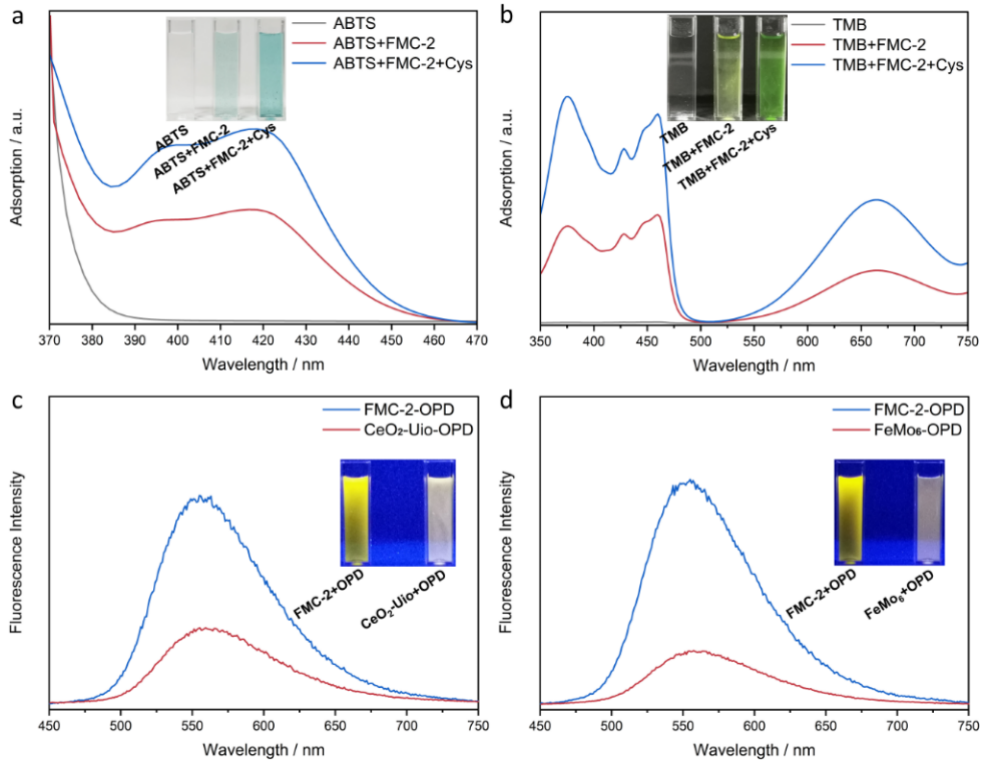

Figure S7. UV-vis spectra and the corresponding optical photographs of (a) ABTS, ABTS-FMC-2 and ABTS-FMC-2-Cys; (b) TMB, TMB-FMC-2 and TMB-FMC-2-Cys (pH=5.5, 5 min, 25 °C); fluorescence curves and corresponding optical photographs of (c) FMC-2-OPD and CeO_2-Uio-OPD; (d) FMC-2-OPD-H_2O_2 and $FeMo_6$-OPD-H_2O_2 (pH=5.5, 5 min, 25 °C).

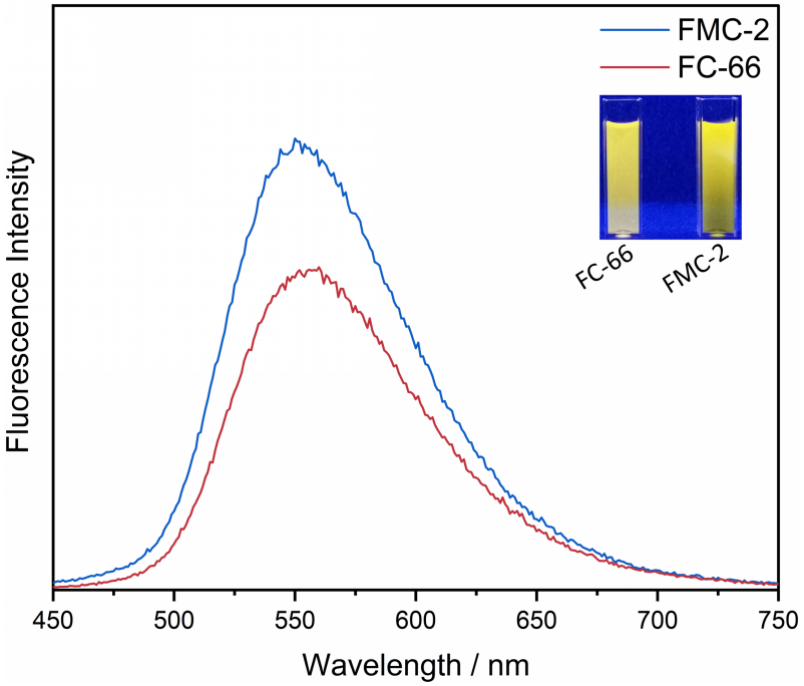

Figure S8. Fluorescence curves and corresponding optical photographs of FMC-2-OPD-O_2 and FC-66-OPD-O_2.

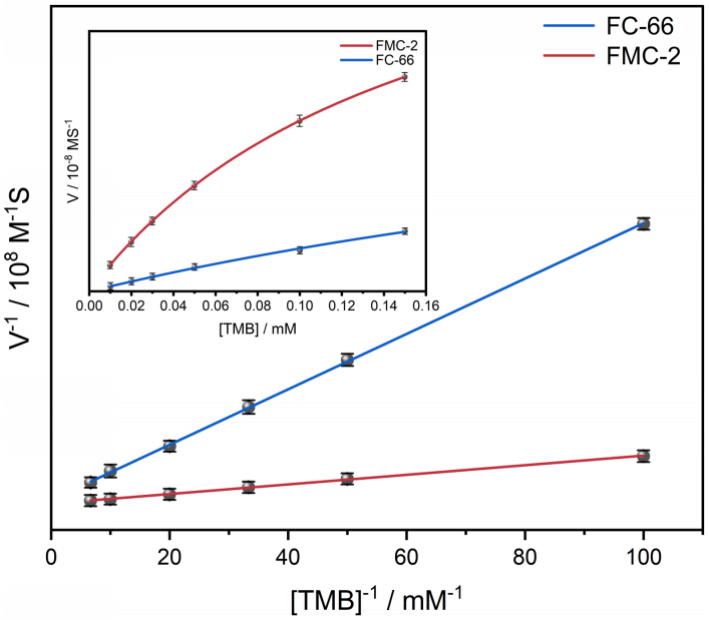

Figure S9. Steady-state kinetics curves of initial reaction rate (*V*) against varying TMB concentration for FC-66 and FMC-2, Lineweaver-Burk plot of 1/*V* against 1/C_{TMB} for FC-66 and FMC-2.

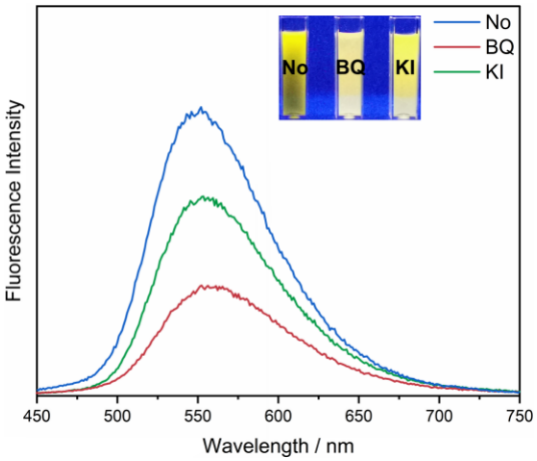

Figure S10 Fluorescence curves and corresponding optical photographs of FMC-2-OPD-O_2 under the effect of 1 mM *p*-benzoquinone (BQ) and potassium iodide (KI) quencher-spiked agent.

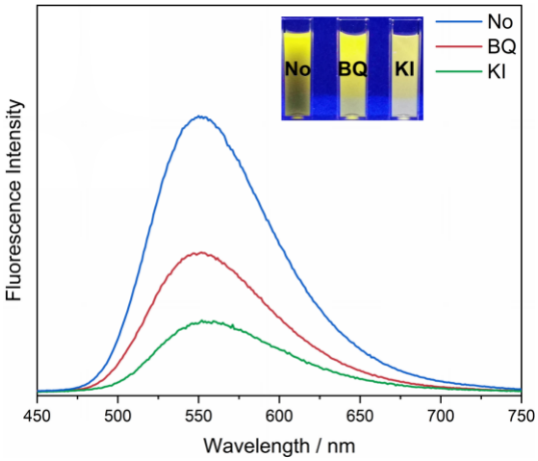

Figure S11 Fluorescence curves and corresponding optical photographs of FMC-2-OPD-O_2-Cys under the effect of 1 mM *p*-benzoquinone (BQ) and potassium iodide (KI) quencher-spiked agent.

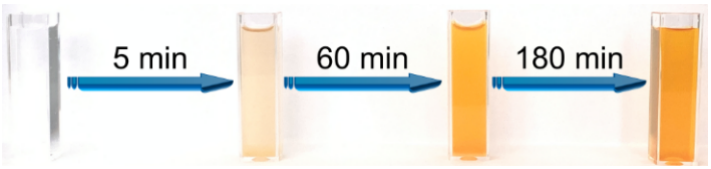

Figure S12 Optical photographs of FMC-2-$TiOSO_4$ over time.

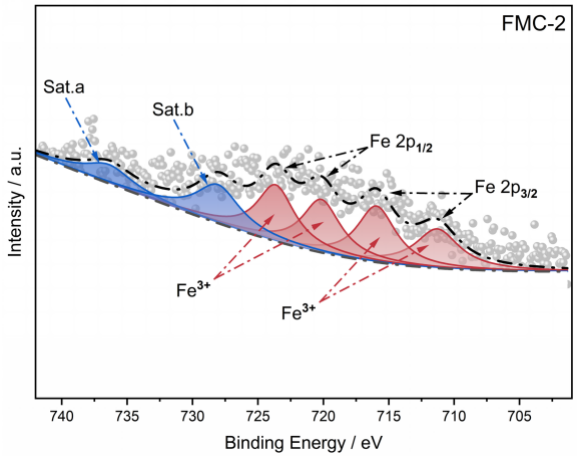

Figure S13. The high-resolution of Fe 2p XPS spectra for FMC-2.

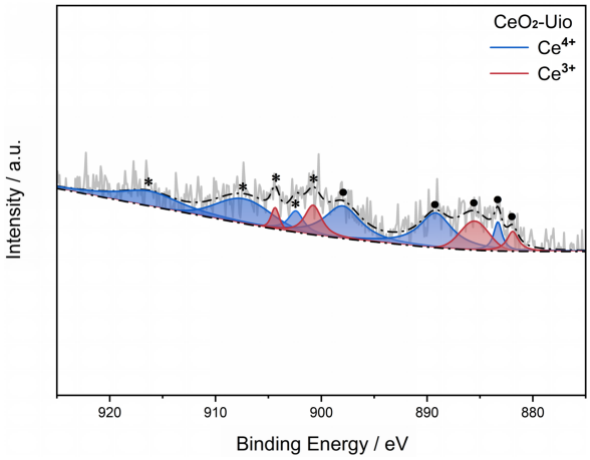

Figure S14. The high-resolution of Ce 3d XPS spectra for CeO_2-Uio, the asterisks assigned to the spin-orbit split $3d_{3/2}$ and circles for $3d_{5/2}$.

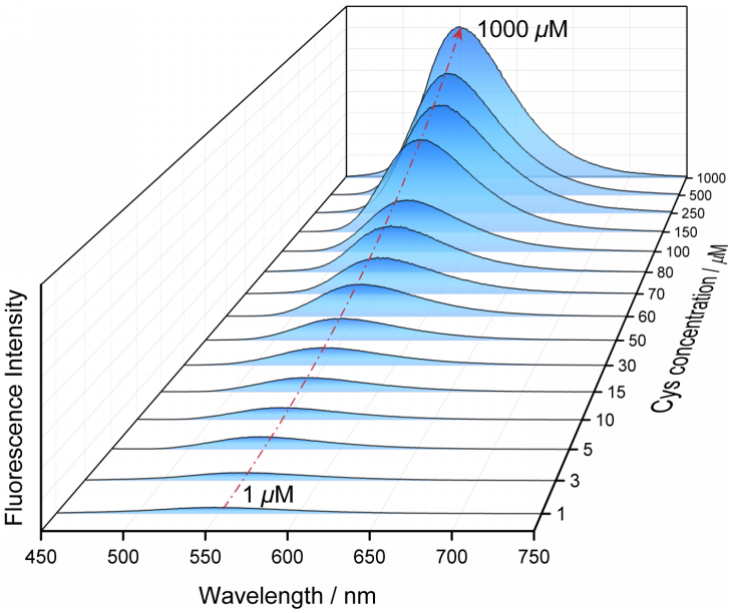

Figure S15 Fluorescence curves of FMC-2 catalyzed oxidation of OPD under the enhancement of different concentrations of Cys.

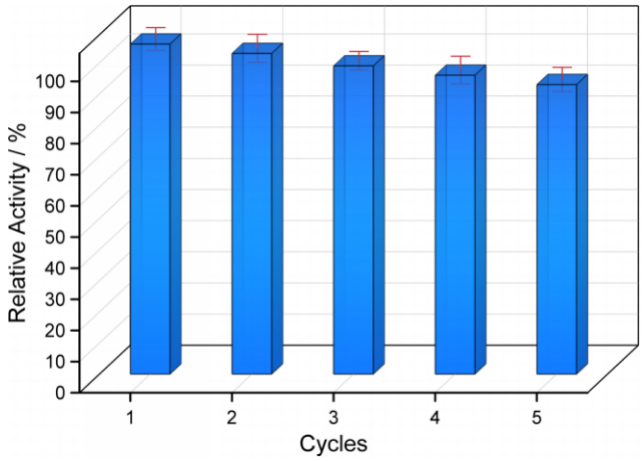

Figure S16 The reproducibility of FMC-2 after repeated cycles.

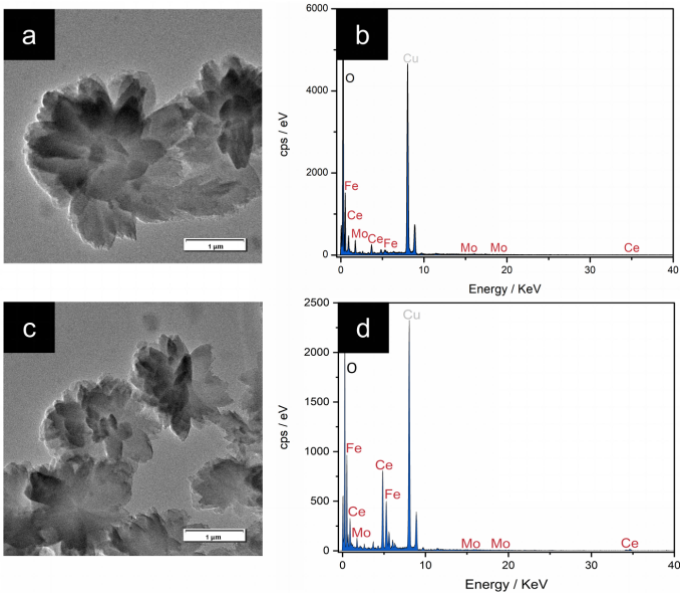

Figure S17 (a) and (b) TEM image and EDS spectrum of FMC-2 before evaluation of self-cascading multienzyme mimic activity, respectively; (c) and (d) TEM image and EDS spectrum of FMC-2 after the reaction, respectively.

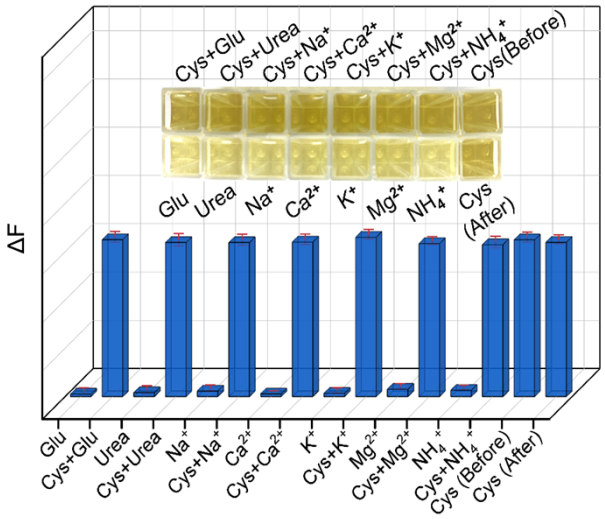

Figure S18 Optical photographs and ΔF of the developed self-cascading multienzyme sensing platform with different analytes. Analytes: 80 μM of K^+, Na^+, Mg^{2+}, Ca^{2+}, NH_4^+, Glu and urea.

Section 2. Supporting Tables

Table S1. Summary of Physicochemical Properties of FC-66 and FMC-n

Sample	S_{BET} ($m^2 \cdot g^{-1}$)	Pore size (nm)	Pore volume ($cm^3 \cdot g^{-1}$)
FC-66	11.61	9.59	0.0508
FMC-1	16.12	12.41	0.0527
FMC-2	35.06	12.10	0.2296
FMC-3	38.86	18.45	0.2345

Table S2. Ce $3d_{3/2}$ and Ce $3d_{5/2}$ components in XPS spectra of FMC-2.

Ionic state	Spin-orbit doublet	Components	BE (±0.1 eV)	FWHM (±0.1 eV)	Ce (III) ratio (%)[1]
Ce(IV)	$3d_{3/2}$	U	906.32	2.88	34 %
		U^{II}	910.78	4.69	
		U^{III}	918.43	8.87	
	$3d_{5/2}$	V	887.25	3.19	
		V^{II}	892.07	4.79	
		V^{III}	901.09	6.60	
Ce(III)	$3d_{3/2}$	U^0	903.94	3.08	
		U^I	908.31	2.88	
	$3d_{5/2}$	V^0	884.67	4.25	
		V^I	889.83	2.91	

Table S3. Ce $3d_{3/2}$ and Ce $3d_{5/2}$ components in XPS spectra of CeO_2-Uio.

Ionic state	Spin-orbit doublet	Components	BE (±0.1 eV)	FWHM (±0.1 eV)	Ce (III) ratio (%)[1]
Ce(IV)	$3d_{3/2}$	U	901.94	2.47	29 %
		U^{II}	908.09	3.42	
		U^{III}	917.06	3.53	
	$3d_{5/2}$	V	883.68	1.91	
		V^{II}	889.26	2.77	
		V^{III}	897.71	2.68	
Ce(III)	$3d_{3/2}$	U^0	900.38	2.32	
		U^I	904.56	2.44	
	$3d_{5/2}$	V^0	881.94	1.78	
		V^I	886.13	2.36	

Table S4. Recoveries of the determination of Cys in human urine samples using the proposed self-cascading multienzyme sensing platform.

Sample	Added (μM)	Measured (μM)	Recovery (%)	RSD (%, n=3)
1	0	9.97 ± 0.19	−	−
	20	29.64 ± 0.13	98.2	1.92
	40	51.28 ± 0.18	102.6	2.03
2	0	11.64 ± 0.16	−	−
	20	30.96 ± 0.15	103.2	2.01
	40	50.56 ± 0.18	101.4	2.14

Section 3. Supporting Schemes

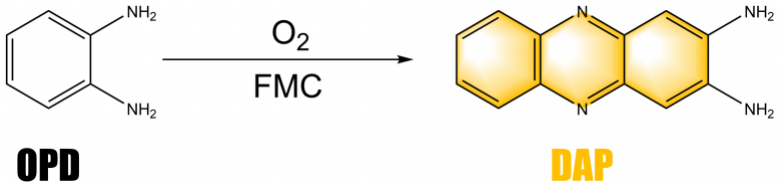

Scheme S1. Catalytic oxidation of OPD by flower-like FMC-3 in the presence of O_2.

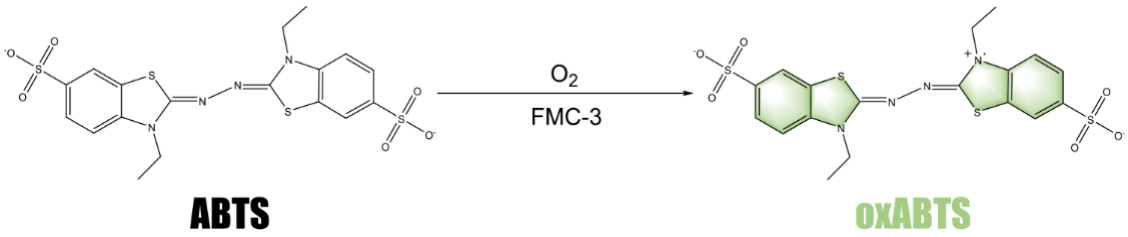

Scheme S2. Catalytic oxidation of ABTS by flower-like FMC-3 in the presence of O_2.

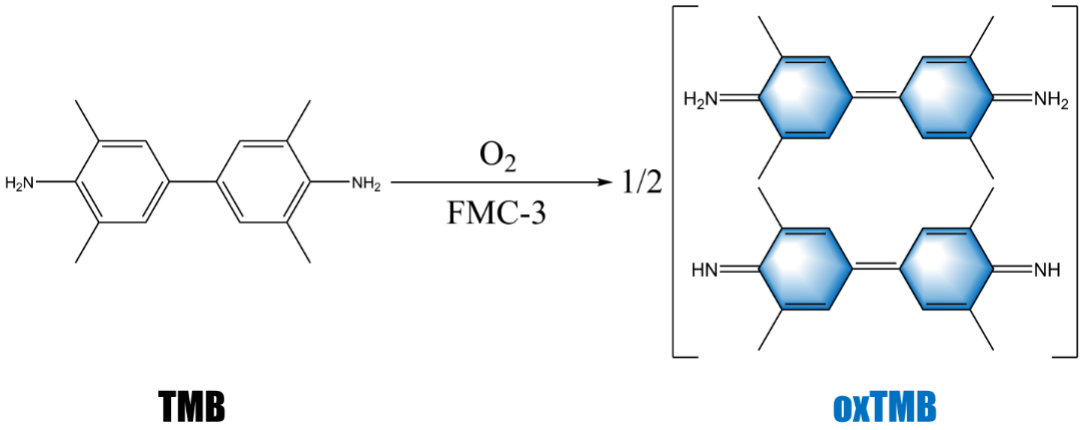

Scheme S3. Catalytic oxidation of TMB by flower-like FMC-3 in the presence of O_2.

$$V_o + O + 2Ce^{3+}_{Lattice} + 3O^{2-}_{Lattice} \longrightarrow 2Ce^{4+}_{Lattice} + 4O^{2-}_{Lattice}$$

Scheme S4. The oxygen vacancy (Vo) action maintains the surface charge of FMC.

References

(1) Beche E, Peraudeau G, Flaud V, et al. An XPS investigation of (La_2O_3) 1-x (CeO_2) 2x $(ZrO_2)_2$ compounds[J]. Surface and interface analysis, 2012, 44(8): 1045-1050.